



Contents lists available at ScienceDirect

Journal of Sea Research

journal homepage: [www.elsevier.com/locate/seares](http://www.elsevier.com/locate/seares)

# Physical processes controlling passive larval transport at the Patagonian Shelf Break Front



Bárbara C. Franco<sup>a,\*</sup>, Elbio D. Palma<sup>b</sup>, Vincent Combes<sup>c</sup>, Mario L. Lasta<sup>d</sup>

<sup>a</sup> Centro de Investigaciones del Mar y la Atmósfera (CIMA)/CONICET-UBA, UMI-IFAECI/CNRS, Buenos Aires, Argentina

<sup>b</sup> Departamento de Física, Universidad Nacional del Sur and Instituto Argentino de Oceanografía (IADO/CONICET), Bahía Blanca, Argentina

<sup>c</sup> Oregon State University, College of Earth, Ocean, and Atmospheric Sciences, Corvallis, USA

<sup>d</sup> Instituto Nacional de Investigación y Desarrollo Pesquero (INIDEP), Mar del Plata, Argentina

## ARTICLE INFO

### Keywords:

Patagonian Shelf Break Front  
Benthic-pelagic interaction  
Stochastic processes  
Patagonian scallop

## ABSTRACT

The largest beds of the Patagonian scallop (*Zygochlamys patagonica*) have been associated with high chlorophyll-*a* concentration observed along the Patagonian Shelf Break Front but there is no supported hypothesis about how this benthic-pelagic connection is maintained. In this work we address the main physical processes driving the benthic-pelagic linkages through oriented numerical experiments derived from a realistic, high-resolution numerical model, and Lagrangian stochastic simulations. The results support the hypothesis of an important dynamical control of the slope current on the fate of surface released passive particles and their subsequent bottom settlement. A high percentage of the particles released at the surface settled over the scallop beds. The particles remaining at the surface layer followed a prevailing NE flow direction with low cross-shelf dispersion. Additional experiments show that the secondary cross-shelf circulation forced by the slope current promotes downwelling and hence the settlement of particles on the westward side (onshore) of the shelf break. The percent of particles settling over the scallop beds exceeded 80% by the addition of vertical stochastic turbulence and tidal forcing. These results highlight the importance of including the vertical diffusivity in particle tracking experiments to better estimate benthic-pelagic interaction processes.

## 1. Introduction

An important task in marine ecosystems is to identify, characterize and quantify the flux of energy between organisms from different marine habitats. A relevant example is the potential dynamical connection (coupling) between the pelagic (surface) and benthic (bottom) layer communities. The structure of several benthic communities have been associated with the phytoplankton production in the overlying water column (Grebmeier and Barry, 1991; Hily, 1991; Graf, 1992), however relatively little is known about the physical factors involved in the interaction between the pelagic and benthic productivity. These physical mechanisms are necessary for communities located at greater depths because they allow the phytoplankton produced in the euphotic zone and associated organic matter to reach such depths (Graf, 1992). Once near or on the seafloor, the organic matter is often initially consumed by suspension feeders (Josefson and Conley, 1997).

Physical processes influencing frontal productivity mediating the benthic-pelagic connection include wind-forced upwelling events, tidal mixing and shelf-break dynamics. Cycles of upwelling and relaxation

generated by the wind can induce areas of higher chlorophyll-*a* (Chl-*a*), where filter-feeders are more abundant and had higher growth rates than in neighboring areas where Chl-*a* is lower (Menge et al., 1997). The downward motion and subsequent establishment of some benthic species has been significantly correlated with these wind events in the US west coast (Wing et al., 1995). The interaction between tidal currents and sloping bottom topography can also generate nutrient flux from the deep region onto shallower areas (i.e. Georges Bank; Tian et al., 2015). Once on the shelf or at the bank edges, tidal mixing redistributes nutrients upward reaching phytoplankton in the near-surface layer and carries particulate matter downward to the benthic communities (Loder et al., 1992). Shelf break fronts separate continental shelf water from slope water and often show high levels of biological productivity. Model results for the Mid Atlantic Bight have suggested that the transverse shelf circulation may be effective in advecting regenerated near-bottom nutrients along frontal isopycnals, potentially reaching the euphotic zone (Gawarkiewicz and Chapman, 1992) and supporting the Chl-*a* maximum found at the surface (Marra et al., 1990). The upward nutrients' flux towards the euphotic zone

\* Corresponding author at: Centro de Investigaciones del Mar y la Atmósfera (CIMA)/CONICET-UBA, Intendente Guiraldes 2160 - Ciudad Universitaria, Pabellón II - 2do, Piso, C1428EGA Buenos Aires, Argentina.

E-mail address: [barbara.franco@cima.fcen.uba.ar](mailto:barbara.franco@cima.fcen.uba.ar) (B.C. Franco).

<http://dx.doi.org/10.1016/j.seares.2017.04.012>

Received 5 October 2016; Received in revised form 24 February 2017; Accepted 27 April 2017

Available online 28 April 2017

1385-1101/ © 2017 The Authors. Published by Elsevier B.V. This is an open access article under the CC BY-NC-ND license (<http://creativecommons.org/licenses/by-nc-nd/4.0/>).

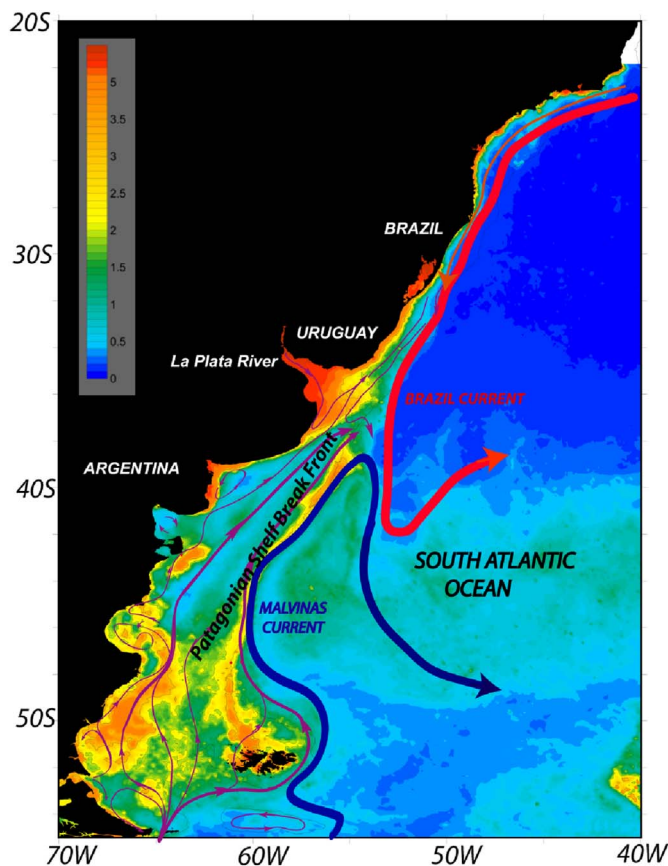


Fig. 1. Schematic of the circulation in the SW Atlantic Ocean. The concentration of surface Chlorophyll- $a$  ( $\text{mg m}^{-3}$ ) obtained with the SeaWiFS radiometer (summer average) is shown in color. Magenta lines indicate the schematic shelf circulation. (For interpretation of the references to color in this figure legend, the reader is referred to the web version of this article.)

might explain the decrease in some species of benthic suspension feeders at the shelf break (Gaston, 1987). In the Celtic Sea the breaking of internal waves at the shelf edge is thought to play an important role on the observed nutrient and Chl- $a$  distributions (Sharples et al., 2009) and possibly the high abundance of benthic communities at the bottom (Heip et al., 2001).

The Patagonian Shelf Break Front (SBF), one of the most productive areas of the world ocean (Acha et al., 2004; Lutz et al., 2010), is located near the edge of the extensive Patagonian shelf and marks the transition between waters of the continental shelf and the cold, nutrient-rich subpolar waters of the Malvinas Current (MC, Fig. 1). The sharpest surface temperature gradients that characterize the front are located along the 200 m isobath (Franco et al., 2008), suggesting a strong topographic control of the frontal system. Shelf break upwelling induced by the interaction of the MC with the bottom topography has been suggested to bring nutrients from the slope current to the euphotic zone sustaining the phytoplankton blooms in the SBF (Matano and Palma, 2008; Combes and Matano, 2014; Valla and Piola, 2015). In-situ (Carreto et al., 1995), and remote sensing measurements (Saraceno et al., 2005; Romero et al., 2006) showed that the SBF is associated with a band of high Chl- $a$  (see Fig. 1), which is a frequently used proxy for phytoplankton abundance. The region of high Chl- $a$  forms a quasi-continuous band located close to the shelf break mainly during austral spring and early summer (Acha et al., 2004; Romero et al., 2006, Fig. 1).

The Patagonian scallop (*Zygochlamys patagonica*) is a suspension feeder bivalve mainly of sedimented phytoplankton and organic matter (Schejter et al., 2002; Mauna et al., 2011) that inhabits soft substrata. The largest beds are located in the bottom of the outer shelf and shelf

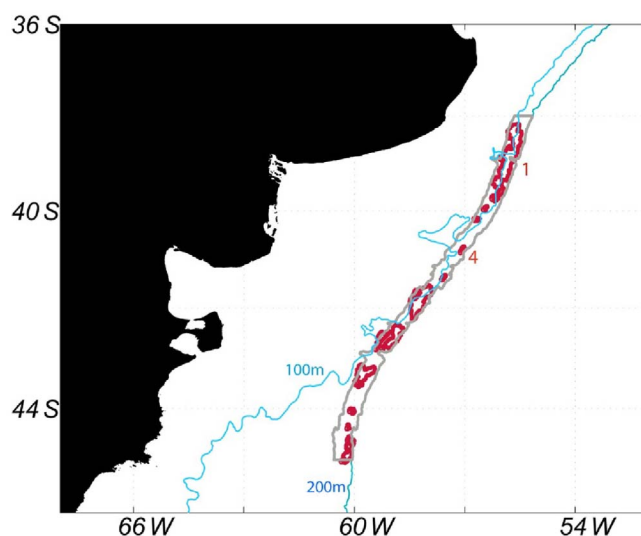


Fig. 2. Location of the largest Patagonian scallop beds (red polygons) (e.g., Bogazzi et al., 2005). Scallop beds 1 and 4 are numbered. The gray heavy line indicates a polygon which extends 50 km western from the location of the particles releases in the SBF. The 100 and 200 m isobaths are shown in blue. (For interpretation of the references to color in this figure legend, the reader is referred to the web version of this article.)

break between 38°S–45°S at depths of  $\sim 80$ –200 m (Fig. 2) nearly matching the surface location of the SBF (Bogazzi et al., 2005; Ciocco et al., 2006). A high concentration of diatoms was reported in gut contents of Patagonian scallops located in the largest bed (number 1, see Fig. 2) (Schejter et al., 2002). The Patagonian scallop is an important economic resource in Argentina, yearly catches of  $\sim 50,000$  t rank this fishery among the most important scallop fisheries in the world (Soria et al., 2016). The fishery, certified as sustainable by the Marine Stewardship Council ([www.msc.org](http://www.msc.org)) in 2006 and 2012, has been carried out since 1996 (Ciocco et al., 2006; Soria et al., 2016).

As the largest Patagonian scallop beds are co-located with the zone of highest primary productivity, it has been suggested that the SBF supplies the planktonic food towards these beds (e.g. Bogazzi et al., 2005; Ciocco et al., 2006; Soria et al., 2016). However, while the latter is in the surface layer the former are found at approximately 150/200 m depth. There is at present no supported hypothesis about how these pelagic-benthic connection (or coupling) is accomplished or what are the main physical processes relating the surface expression of the SBF with the scallop beds at the outer shelf and shelf break. In this study we analyze the dynamical linkages between the surface and bottom layer of the SBF employing a suite of Lagrangian particle tracking simulations built on the results of a three dimensional hydrodynamical model.

## 2. Material and methods

### 2.1. Hydrodynamic numerical model

The Lagrangian particle tracking approach, explained in the following section, uses the outputs of a high-resolution ocean hydrodynamical model developed by Combes and Matano (2014). To summarize, the ocean model is the Regional Ocean Modeling System (ROMS\_AGRIF version; Debreu et al., 2012), which is a three dimensional, free surface, hydrostatic, eddy-resolving primitive equation ocean model. The model uses a high-resolution “child” grid embedded into a coarser-resolution “parent” grid. The parent grid encompasses the entire southern hemisphere. It has a spatial resolution of  $1/4^\circ$  with 40 terrain-following vertical levels. The child domain extends from  $82^\circ\text{W}$  to  $41^\circ\text{W}$  and from  $64^\circ\text{S}$  to  $20^\circ\text{S}$ , with a spatial resolution of  $1/12^\circ$  and 40 vertical levels. The bottom bathymetry is derived from ETOPO1 (Amante and Eakins, 2009). At the northern boundary, the parent grid is nudged towards the monthly mean climatology from the Simple Ocean Data Assimilation

model (SODA; Carton and Giese, 2008). SODA also provides the initial condition. At the surface the model is forced with monthly mean climatology wind stress from ERA\_Interim (Dee et al., 2011) and fresh water and heat fluxes from the COADS (da Silva et al., 1994) data sets. The model forcing also includes a  $23,000 \text{ m}^3 \text{ s}^{-1}$  discharge from La Plata River ( $34.4^\circ\text{S}$ ), and the  $M_2$  tidal component (Egbert and Erofeeva, 2002). The ocean model provides the 3 day-averaged three-dimensional currents and vertical diffusivity fields to be used by the Lagrangian particle tracking model. More detailed technical description of the model configuration, including the spin-up procedure and implementation of tidal, wind, heat and freshwater forcing, river discharge, boundary conditions and mixing parameterizations, as well as a comparison of the model results with observations can be found in Combes and Matano (2014).

## 2.2. Particle tracking model

The particle tracking algorithm computes the trajectories of passive particles based on the following equation:

$$\frac{d\mathbf{X}}{dt} = A(\mathbf{X}, t) + S_v(\mathbf{X}, t) + S_h(\mathbf{X}, t) \quad (1)$$

where  $\mathbf{X}$  is the 3D position of the particle,  $A$  is the advection term and  $S_v$  and  $S_h$  are sub-grid scale turbulent stochastic terms in the vertical and horizontal directions respectively. The realistic hydrodynamic ocean model provides the tracking algorithm with the 3D velocities ( $A$ ), the vertical diffusion coefficient ( $K_v$ ) on which the formulation of the vertical stochastic term ( $S_v$ ) is based, and the horizontal diffusion coefficient ( $K_h$ ) for the computation of  $S_h$ .

To integrate the stochastic differential Eq. (1) we used the Larval Transport Lagrangian Model (LTRANS, Schlag et al., 2008) implemented with a higher order stochastic numerical scheme (Franco et al., 2015). The stochastic displacement (sub-grid scale) of the particles was calculated using a time step of 4 s. This relatively small time step is recommended to avoid artificial vertical accumulations of particles in situations involving nonhomogeneous vertical diffusivity (Ross and Sharples, 2004). LTRANS is endowed with a sophisticated scheme of interpolation and smoothing of the vertical diffusivity field (Tension Splines) that does not add inflection points and preserves the monotonicity and convexity of the data.

Usually studies using coastal circulation models regard the coefficient of horizontal diffusion ( $K_h$ ) either constant or null in the simulations. However, in regions with eddies or strong currents, which could induce intense turbulent mixing, the stochastic behavior (sub-grid scale) might also be considered in the horizontal for particle tracking. LTRANS contains a provision for a horizontal turbulent coefficient to simulate the stochastic horizontal diffusion using a Gaussian random flight process with additional displacements ( $\partial x$  and  $\partial y$ ) in the form of a “naive” random walk (Visser, 1997):

$$\partial x, \partial y = 2K_h^{1/2} \partial W_t \quad (2)$$

where  $\partial W(t)$  is one incremental Wiener process.

Larval transport and dispersion can also be affected by its buoyancy (settling or terminal velocity) and/or its individual behavior (i.e., swimming, mortality) particularly in small scales. In our simulations we assumed that individuals have no swimming ability or biological attributes, which may be appropriate for a monthly time scale. Therefore the particle's movement is completely dominated by advection and turbulent diffusion processes. This condition is not too restrictive if we consider that swimming speeds of phytoplankton are of the order of 0.1 to 0.5 mm/s (Ross and Sharples, 2008) while vertical velocities larger than 8 mm/s have been estimated for the SBF (Valla and Piola, 2015).

More than 50,000 passive particles were released from the surface layer ( $0 > z > -5 \text{ m}$ ) along the climatological position of the SBF

(200 m isobath) and over the latitudinal extension of the beds  $38^\circ\text{S}$ – $45^\circ\text{S}$ . A total of 8,456 particles were released every 5 days and tracked for each selected month (30 days). The simulations were set-up during the months of spring and early summer, when a high phytoplankton biomass is associated with the SBF. The analysis of the particle tracking experiments was divided into two distinct groups of statistics. In the first group we computed the number of particles that reach the bottom at the end of each monthly simulation. Particles (“larvae”) were recorded as “settled” if they arrived within any of the user-specified settling or habitat polygons. Note that in this context settling does not refer to the particle terminal (Stokes) velocity but to the attachment of a specific particle to the bottom. The model was set up for the settlement (that is bottom establishment) of the particles that reach the bottom inside of the scallop bed areas. Each scallop bed was configured as a polygon by using its boundary positions (longitude, latitude) indicated in Fig. 2. To determine if the particle was inside or outside of an irregularly shaped polygon, we employed the technique recommended by Schlag et al. (2008). Particles reaching the bottom outside of the beds were free to move with the currents. We also analyzed differences in the particle horizontal dispersion behavior when adding a horizontal random-walk with two values of  $K_h$  (1 and  $50 \text{ m}^2 \text{ s}^{-1}$ ), which are reasonable for the shelf break region (Ledwell et al., 1998; Thorpe, 2005). We configured 10 distinct stochastic simulations for each month. In the second group of experiments we tracked the position of passive particles that remain in the surface or euphotic layer ( $0 > z > -10 \text{ m}$ ) during the same period. The purpose of these simulations was to monitor the surface dispersion of the particles as a proxy of food availability for the scallop beds.

## 2.3. Dispersal kernel (2D)

To characterize the main area of dispersion of the particles that remain in the euphotic layer at the end of each monthly particle-tracking experiment we computed the dispersion ellipses (2D dispersal kernel). The configuration of the dispersion ellipses involves averaged horizontal mean positions of each particle and indicates the areas of highest concentration of particles located in the surface layer at the end of each monthly simulation. Each one of these areas represents regions of high quantity of planktonic food (e.g., phytoplankton, organic matter) originated in the SBF. A Principal Component Analysis (PCA) was used to compute the dispersion ellipses. The distortion of a particle group was quantified by a horizontal covariance matrix, the components of which account for the covariance between particle displacements relative to their centre of mass.

## 2.4. Dynamics of coupled benthic-pelagic processes

Finally, we investigated the potential dynamical drivers of the benthic-pelagic interaction between the Patagonian SBF and the bottom of the outer shelf and shelf break region. To address this problem we developed a suite of four additional particle tracking experiments where we neglected the horizontal sub-grid scale turbulence ( $K_h$ ) and we analyzed in turn particular forcing mechanisms. The first two experiments were designed to access the importance of vertical advection without the inclusion of sub-grid scale stochastic turbulence ( $K_v = 0$ ). In EXP1 the main forcing mechanism at the shelf break in the hydrodynamical model was the slope current, whereas in EXP2 tidal forcing was also included. The remaining tracking experiments included the sub-grid scale vertical turbulence algorithm without (EXP3) and with tidal forcing added (EXP4). The settlement polygon extended 50 km to the west from the location of the particles release site (SBF) used in the previous numerical simulations (200 m isobath) (Fig. 2). This is in correspondence with a previous study showing that the latitudinal band of high Chl-*a* develops mainly along the western side of the SBF (e.g. Romero et al., 2006).

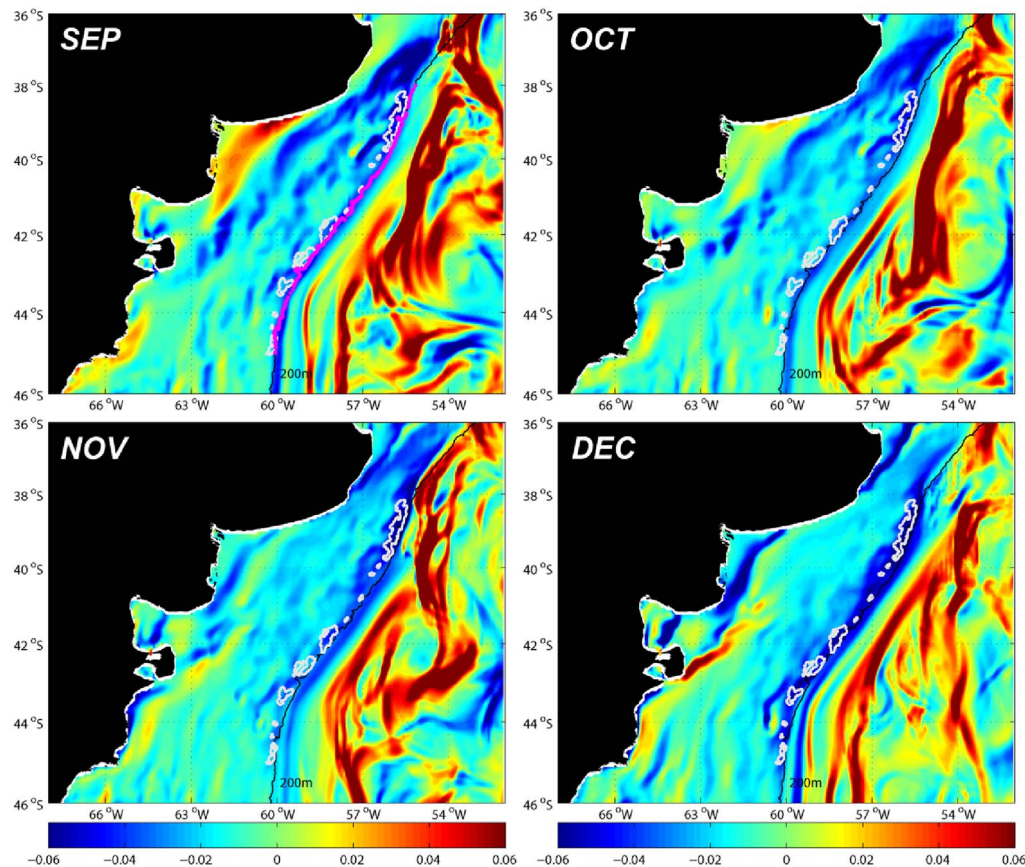


Fig. 3. Monthly mean of cross-shelf break SST gradients (gSST,  $^{\circ}\text{C km}^{-1}$ ). Location of the largest Patagonian scallop beds (gray polygons) along the outer shelf and shelf break are shown. The area of particle release at the surface of the SBF is shown by a thick line (magenta) in the top left panel (September). The 200 m isobath is shown as a black line. (For interpretation of the references to color in this figure legend, the reader is referred to the web version of this article.)

### 3. Results

#### 3.1. Characterization of the SBF

The monthly position of the SBF was characterized by calculating the cross-shelf break gradient of SST (Sea Surface Temperature) from the realistic model results according to Franco et al. (2008) ( $\text{gSST } ^{\circ}\text{C km}^{-1}$ , Fig. 3). As the SBF develops at the transition from warm shelf waters to colder MC waters, it is associated with negative maximum cross-shelf break SST gradients near the shelf break. The model reproduced a band with negative maximum cross-shelf break SST gradients mainly nearly the 200 m isobath (shelf break, Fig. 3). Our analysis of the modeled gSST also showed the surface expression of the fronts associated with the two main branches of the MC (in November and December in Fig. 3) (Franco et al., 2008). The northernmost and largest scallop bed matches the location of the highest negative maximum of gSST from the outer shelf to the 200 m isobath.

#### 3.2. Particle tracking experiments

##### 3.2.1. Bottom settlement

The monthly number of particles settled at each Patagonian scallop bed for each of the  $K_h$  values was calculated as the mean number of particles recorded by the 10 different stochastic simulations (Fig. 4). A higher value of horizontal diffusivity can induce a higher horizontal dispersion of particles and hence they could reach surrounding areas over the largest beds.

For every monthly simulation using  $K_h = 50 \text{ m}^2 \text{ s}^{-1}$  a higher number of particles settled in the largest bed (number 1, see Fig. 2). Although this difference is not seen in October in Fig. 4 the concentra-

tion of particles settled for the simulations using  $K_h = 1$  and  $50 \text{ m}^2 \text{ s}^{-1}$  was of 5368 and 6509, respectively. In addition, when  $K_h = 50 \text{ m}^2 \text{ s}^{-1}$  was used particles settled over a significantly larger area in the east side of this bed and some particles also settled in its west side from October to December (not shown). Previous studies reported a  $\delta^{13}\text{C}$ -enriched phytoplankton accumulation in the east side of this scallop bed, while in surrounding areas (west side of the bed) more degraded organic matter becomes important in the trophic web (Mauna et al., 2011).

The largest differences using  $K_h = 1 \text{ m}^2 \text{ s}^{-1}$  compared to  $K_h = 50 \text{ m}^2 \text{ s}^{-1}$  were observed in the largest scallop bed (number 1) during December with a total of only 3256 particles settled and in scallop bed number 4 where 5096 particles settled during September. The results showed that more than a half of the particles released at the surface along the SBF can reach the bottom and settle over the scallop beds; the highest percentage of settlement is of 62% (December,  $K_h = 50 \text{ m}^2 \text{ s}^{-1}$ ) and the lowest 52% (September,  $K_h = 1 \text{ m}^2 \text{ s}^{-1}$ ).

##### 3.2.2. Surface dispersion

Dispersion ellipses were defined for the experiments which used  $K_h = 50 \text{ m}^2 \text{ s}^{-1}$  to determine the areas of higher dispersion in the surface layer. The results showed that the dispersion of the particles agrees with the location of the SBF and the circulation on the Patagonian shelf and slope. The SBF and the strong N-NE flow of the MC prevented a higher offshore dispersion of the particles drifting at the surface. North of  $\sim 38^{\circ}\text{S}$  the particles were dispersed following the circulation generated in the Brazil-Malvinas Confluence (BMC) region. The highest percentage (11%) of particles reaching the BMC region and advected offshore towards the deep ocean was recorded by the simulations using  $K_h = 1 \text{ m}^2 \text{ s}^{-1}$  during December. In November a very low concentration (1.2%) of particles located at the surface drifted

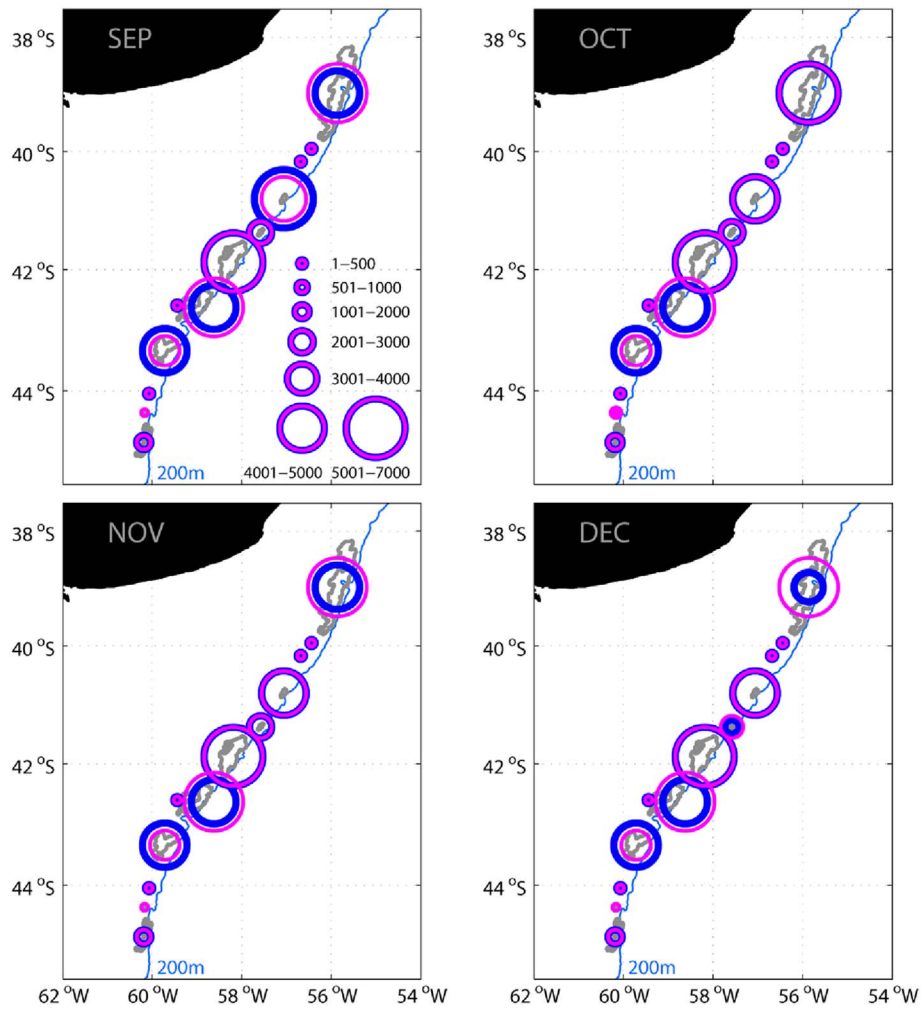


Fig. 4. Number of particles settled at each Patagonian scallop bed for each month. Results of simulations for  $K_h = 1 \text{ m}^2 \text{ s}^{-1}$  are shown by a thick blue circle and for  $K_h = 50 \text{ m}^2 \text{ s}^{-1}$  by a thin magenta circle. The scale for the number of particles settled is shown in the upper left panel (September). The 200 m isobath is indicated as a thin blue line. (For interpretation of the references to color in this figure legend, the reader is referred to the web version of this article.)

further north forced by the mean advection reaching  $\sim 36^\circ\text{S}$  in the outer shelf (Fig. 5). Surface particles were located over the shelf and west of the 200 m isobath mainly north of  $41^\circ\text{S}$  (Fig. 5, inserts located at the bottom right of each panel). A higher dispersion of surface particles onto the continental shelf was recorded by the experiments using  $K_h = 50 \text{ m}^2 \text{ s}^{-1}$ . Frequent intrusions of MC waters into the outer shelf could occur through horizontal divergence of the flow over the slope and/or by upwelling. Once particles are dispersed by intrusions from flows onto the shelf and outer shelf they can remain in the surface or can be transported to the bottom. We suggest that such intrusions from the slope onto the outer continental shelf could explain the high settlement of particles in bed number 4 (located  $\sim 40.8^\circ\text{S}$ ). Our results also showed that the particles that remained in the surface layer at the end of each monthly simulation were not located over bed number 1 (Figs. 2 and 5).

The results show a significantly lower percentage of particles in the surface when compared with the settled particles in the scallop beds. The percent of particles remaining at the surface increases from September ( $\sim 8\%$ ) towards early summer (December, 20%) for  $K_h = 1 \text{ m}^2 \text{ s}^{-1}$ . The higher stratification in the surface layers could be hindering the vertical transport of particles located in the surface. The same seasonal tendency was recorded using  $K_h = 50 \text{ m}^2 \text{ s}^{-1}$  with a slight difference in the percentage of particles located at the surface.

### 3.3. Physical processes affecting benthic-pelagic interactions at the SBF

To determine the relative contribution of the slope current, tidal forcing and sub-grid scale stochastic turbulence on the particle settlement over the scallop beds we conducted a series of four additional sensitivity experiments (see Section 2.4). Since the highest particle settlements on scallop beds were observed in November, the velocity fields of this month were selected to carry out the corresponding tracking experiments. In EXP1 41% of the particles released at the surface settled inside the selected polygon (the gray rectangle in Fig. 2) showing the effect of the (secondary) transverse circulation associated with the slope current, generating upwelling on the eastern side of the SBF and downwelling on the western side (see Fig. 9, Matano and Palma, 2008). These vertical fluxes can carry nutrients to the surface east of the front and organic matter to the bottom west of the front. When tidal forcing was included in the ocean model (EXP2) the results showed a slight enhancement on benthic-pelagic coupling with 49% of the particles settled at the selected polygon. EXP3 and EXP4 highlight the importance of the sub-grid scale stochastic turbulent processes in the vertical. In EXP3 71% of the particles settled boosted by the intense vertical mixing ( $K_v$ ) generated by the interaction between the slope current with a steep topography (Fig. 6a). The simultaneous addition of tidal forcing (EXP4) intensified the vertical mixing processes ( $K_v$ ) in the bottom and upper layers over the outer shelf and shelf break (Fig. 6b) resulting in a significant additional increase in turbulent vertical transport and settlement of particles (82%). In summary, the cross-

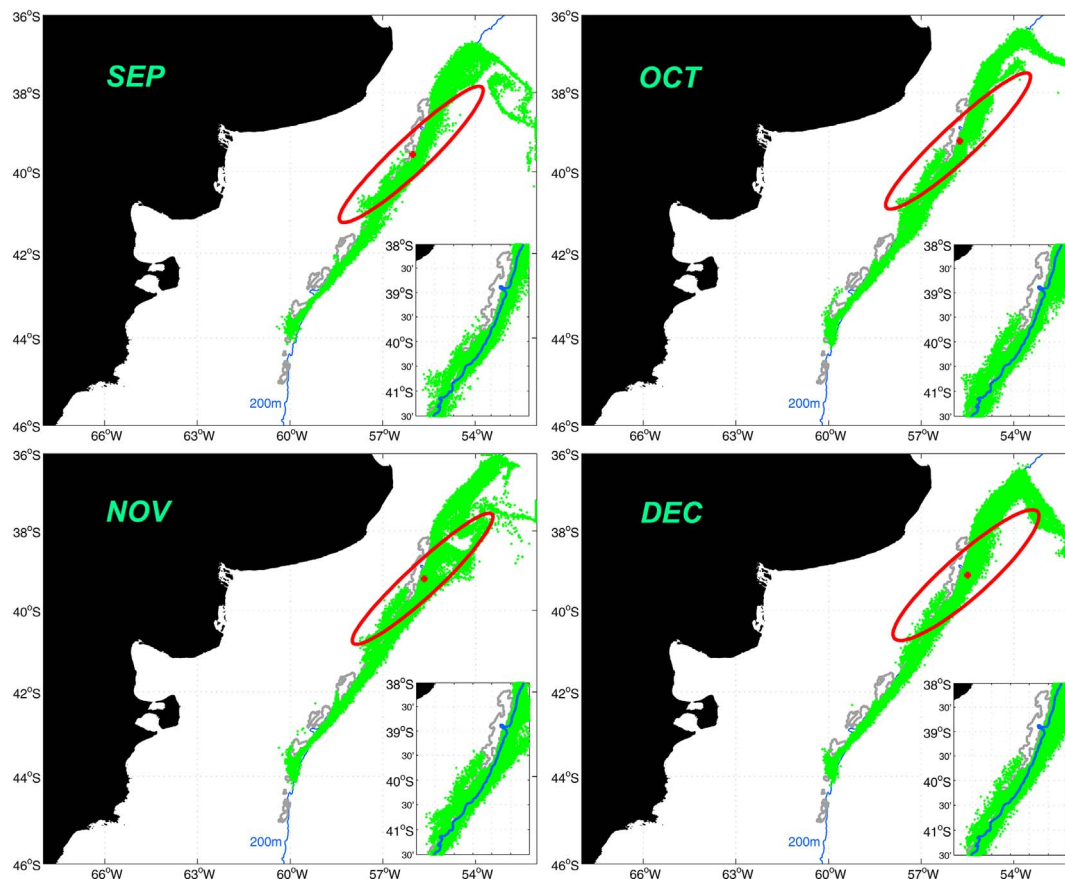


Fig. 5. Location ( $x, y$ ) of the particles in the surface layer ( $0 > z > -10$  m) at the end of each monthly experiment (green points). The positions are the mean location from 10 trials. Dispersion ellipses (2D) of the particles are shown in red. The area of intrusions of MC waters onto the continental shelf near  $41^{\circ}\text{S}$  can be seen by an insert in the right bottom of each panel. The experiments used  $K_h = 50 \text{ m}^2 \text{ s}^{-1}$ . The 200 m isobath is shown as a thin blue line. (For interpretation of the references to color in this figure legend, the reader is referred to the web version of this article.)

shelf circulation induced by the slope current at the shelf break connects the surface layer with the bottom layer but the interaction process was markedly enhanced by stochastic turbulent mixing (also induced by the slope current in the subsurface layers) and the inclusion of tidal forcing.

#### 4. Discussion

In this study we have investigated the main physical processes responsible for the horizontal advection and vertical transport of passive particles (resembling surface plankton) in the SBF employing the results of a 3D high resolution hydrodynamic numerical model. The model reproduced the surface expression of the two main branches of the MC associated with a band of negative maximum cross-shelf SST gradients mainly near the shelf break. These features matched well with the analysis of satellite SST by Franco et al. (2008) and other studies that characterize the SBF climatological position and the multiple branches of the MC (Piola et al., 2013; Valla and Piola, 2015).

Using the hydrodynamic model velocity fields, a large number of passive particles were then released at the surface along the SBF climatological position and over the latitudinal extension of the scallop beds and tracked in time using a Lagrangian stochastic algorithm. The particle tracking model showed that the surface dispersion of the particles agrees with the location of the SBF and the circulation on the Patagonian shelf and slope with weak horizontal dispersion. Intrusions of MC waters onto the continental shelf near  $41^{\circ}\text{S}$  were previously reported (Piola et al., 2010). Their work suggests that the intrusions of cold, nutrient-rich waters of the MC are important in promoting the local development of phytoplankton near  $41^{\circ}\text{S}$ . Our

results showed the occurrence of a higher concentration of particles (resembling ‘phytoplankton’) over this area mainly in September and October (Fig. 5, inserts).

Once the particles are dispersed by intrusions onto the shelf they can remain in the surface layer or can be transported to the bottom. The tracking simulations have shown that in fact  $> 60\%$  of the particles released at the surface settled in the scallop beds after one month. This percentage is almost independent of the month of release, an additional confirmation of the strong control of the slope current on the shelf break dynamics. Sensitivity experiments without stochastic forcing indicated that a large part of the downward motion of the surface particles can be attributed to the (secondary) transverse circulation associated with the slope current. This result is in agreement with the idealized model of Matano and Palma (2008) where the northward motion of a slope current generates upward motion on the eastern side of the shelf-break and downwelling motion on the western side. Such vertical fluxes can provide nutrients to the euphotic layer east of the front and organic matter to the bottom layers west of the front. In the realistic model, permanent intrusions of MC waters could occur through horizontal divergence of the flow over the slope and/or by upwelling. We suggest that such intrusions from the slope onto the continental shelf could explain the high settlement of particles in scallop bed number 4 (located  $\sim 40.8^{\circ}\text{S}$ ).

The bottom settlement of particles is enhanced by the addition of vertical stochastic turbulence and tidal forcing exceeding 80% of the number of particles released at the surface. The interaction of the slope current with a steep topography intensifies the vertical mixing in the subsurface and bottom layer but the inclusion of the semidiurnal tides enhance the mixing along the water column and therefore the vertical

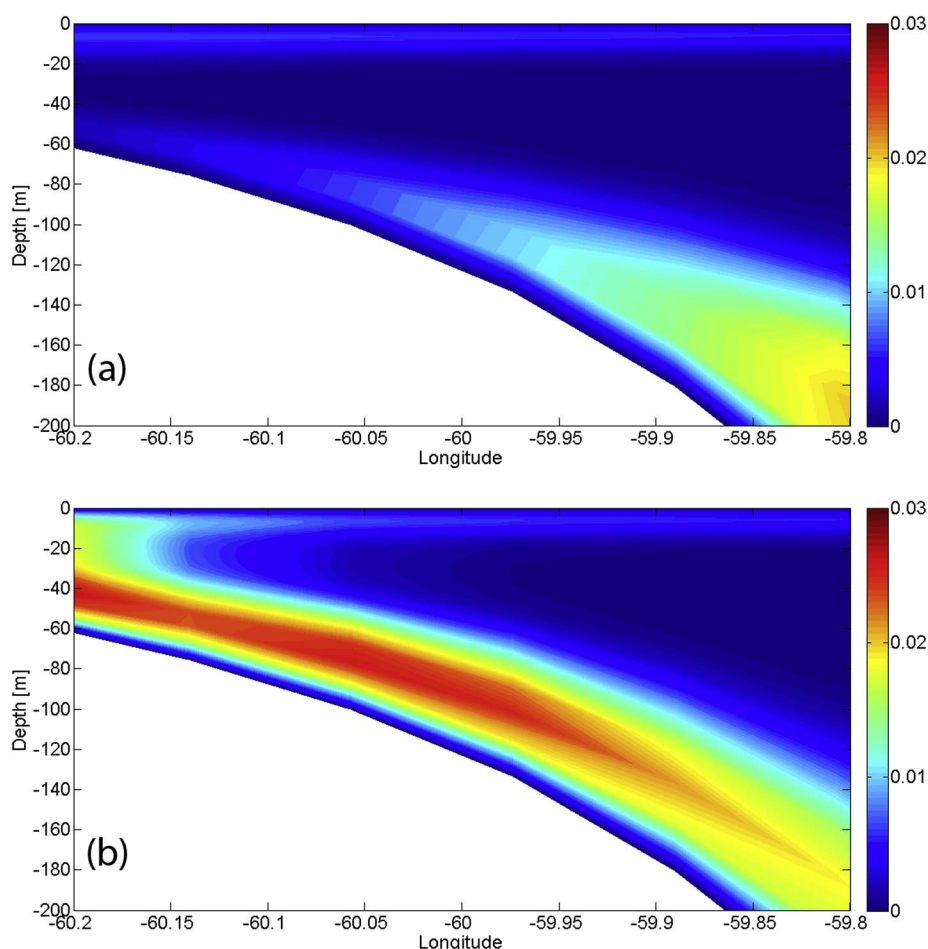


Fig. 6. Cross section of vertical diffusivity ( $K_v$ ,  $\text{m}^2 \text{s}^{-1}$ ) for experiments (a) EXP3 and (b) EXP4 near  $44^\circ\text{S}$ . (For interpretation of the references to color in this figure legend, the reader is referred to the web version of this article.)

coupling (Fig. 6). Simpson and Souza (1995) reported that semidiurnal oscillations in the stability of the water column are forced mainly by tidal advection when horizontal movements interact with vertical density gradients generating disturbances in the stratification. In the SBF semidiurnal amplitudes in the cross-shore (U) component of the velocity near  $44^\circ\text{S}$  of about 8–11 cm/s were previously reported along the water column, from 10 m depth until 160 m, in a mooring deployed during the early spring of 2005 (Franco, 2013). This periodical semidiurnal breakdown of the vertical stratification in the area of surface frontal variability can further contribute to flux particles initially located at the base of the surface mixed layer downward and inshore, following front isopycnals down to the seafloor.

To illustrate this process at the SBF we show in Fig. 7a the cross-shelf structure of observed density anomaly and fluorescence (a proxy for Chl-*a*) derived from observations collected near  $44^\circ\text{S}$  on 15–16 October 2005 (early spring, see Charo and Piola, 2014). The pycnocline is located around 50 m depth and the SBF structure is associated with a weakening in vertical stratification over the shelf break as determined by the Brunt–Väisälä frequency,  $N < 2$  cph (Fig. 7a). High fluorescence is observed at the shelf break, with highest concentration in the upper 50 m of the water column, and relatively high concentration ( $> 3 \text{ mg m}^{-3}$ ) extending vertically beyond 100 m depth over the outer shelf and shelf break, east of the 200 m isobath (Fig. 7b). Observations of high Chl-*a* concentration from the surface of the shelf break down to the bottom mixed layer, and distributed almost homogeneously in the water column (slightly decreasing up to 80 m depth) are also shown by Carreto et al. (2016).

The dynamics of the Patagonian SBF and its related benthic-pelagic interaction processes have some similarities with the Northeastern Peak

on Georges Bank. Modeling studies in this region indicate that much of the nutrient supply to the surface frontal waters is driven by short but intense mixing events during each semidiurnal tidal cycle (Franks and Chen, 1996), with the steep slopes of the bank generating on-bank residual flows that allow the transport of bottom layer nutrients to the front supporting a high primary productivity. The densest sea scallop (*Placopecten magellanicus*) beds on the seafloor of Georges Bank tend to lie under the region where the pycnocline intersects the bottom and therefore receive more particulate matter downward. As the tide moves the tidal fronts back and forth, the scallop beds can be under either stratified or well-mixed waters (Pringle and Franks, 2001). Our results suggest that in the SBF the main mechanism of nutrient supply to the upper layers is the transverse circulation and vertical mixing generated by a strong equatorward western boundary current (the MC; Matano and Palma, 2008). The inclusion of tidal forcing in the experiments, however indicates that some nutrients may reach the SBF and the bottom by the periodic semidiurnal motion induced by the tides at the shelf break.

## 5. Summary and conclusions

The analysis of the modeled particle trajectories released at the surface of the SBF in several numerical experiments allowed us to estimate the surface larval dispersal routes, the degree of interaction between the surface and the bottom layer, and the main physical processes involved in this interaction.

The model results support the hypothesis that the MC is the dominant circulation mechanism at the shelf break and thus predominantly determines the passive larval behavior. The strong N-NE flow of

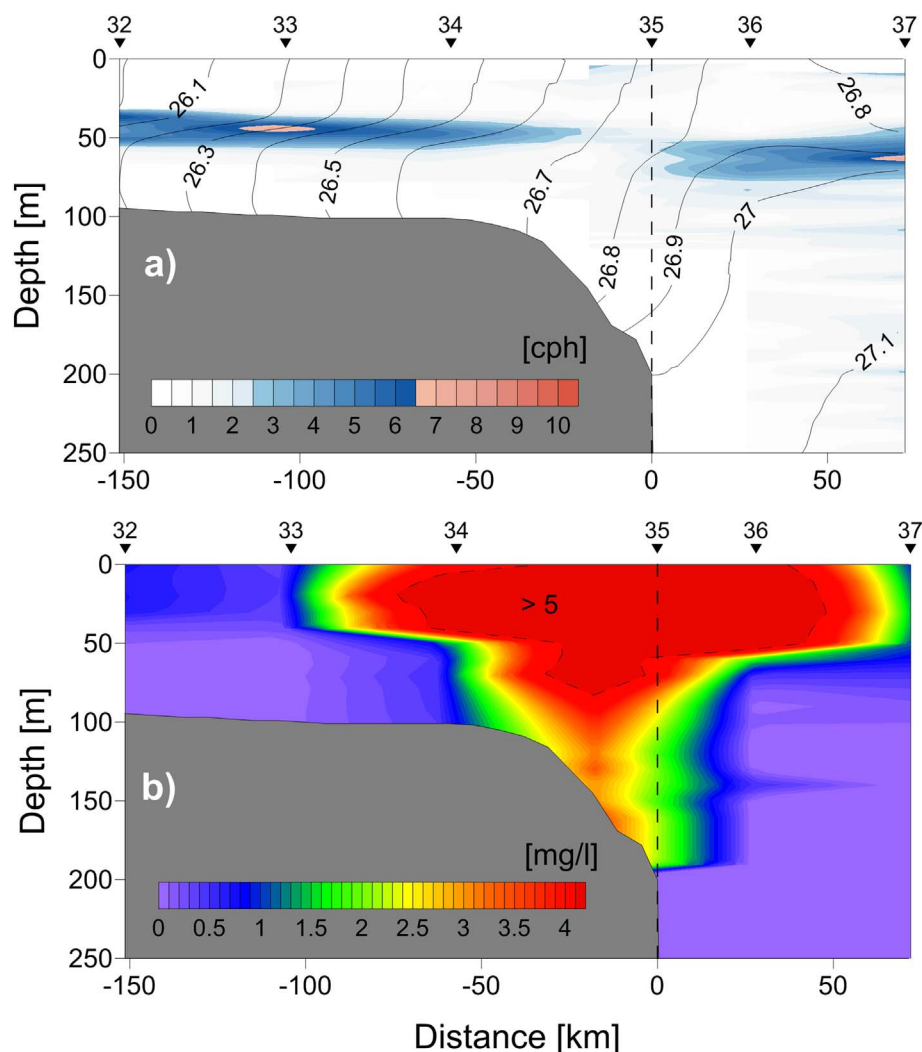


Fig. 7. (a) Brunt-Väisälä frequency (cph) section across the Patagonian shelf near 44°S collected in October 2005. Contours represent potential density in  $\text{kg m}^{-3}$ . (b) Chlorophyll-a (Chl-a) concentration ( $\text{mg m}^{-3}$ ) derived from fluorescence observations. The dashed line indicates the position of the 200 m isobath, which is used as the origin along the x axis. Redrawn from Valla and Piola (2015). (For interpretation of the references to color in this figure legend, the reader is referred to the web version of this article.)

the MC does not allow significant cross-shore dispersion of the particles at the surface. At the end of the simulation some of the particles that remain in the surface layer reached the BMC region and are advected offshore towards the deep ocean. Once the particles are dispersed by intrusions onto the shelf and outer shelf they can remain in the surface or can be transported to the bottom.

The same experiments have shown that > 60% of the particles released at the surface are able to settle at the bottom in the scallop beds after one month. This percentage is almost independent of the month of release, an additional confirmation of the strong control of the MC on the shelf break dynamics. The downward motion of the particles in the western (onshore) side of the shelf-break is favored by the secondary circulation resulting from the interaction between the MC and the bottom topography. Sensitivity experiments also show that the contact of the surface particles with the bottom is enhanced by the addition of sub-grid scale stochastic turbulent processes in the vertical and the semidiurnal tidal component in the boundary forcing.

Overall our results emphasize the importance of the physical forcing in the linkage processes between the pelagic and benthic communities in the SBF region. Such processes could supply planktonic food to the scallop beds and could mediate the survival of the epibenthic community which inhabits the bottom over the shelf break. Improving our knowledge about these interactions is crucial to provide a better understanding about fluctuations in the recruitment of a wide group

of marine species. This study, based on the tracking of passive particles is a first step in that direction.

#### Acknowledgments

BCF was supported by a Ph.D. Scholarship from Consejo Nacional de Investigaciones Científicas y Técnicas (CONICET, Argentina). Support for ED Palma came from Agencia Nacional de Promoción Científica y Tecnológica (ANCYPT-Grant PICT12-0467) and Universidad Nacional del Sur (Grant 24/F066). The work was carried out with the aid of a grant from the Inter-American Institute for Global Change Research (IAI) CRN2076, which is supported by the US National Science Foundation (Grant GEO-0452325). Additional support came also from an IAI grant CRN3070 (VOCES), (Grant GEO-1128040). The critical reading of Oscar Iribarne and Alberto Piola is kindly appreciated. We thank Daniel Valla for his help in composing Fig. 7. The paper benefited substantially from suggestions given by the anonymous reviewers.

#### References

- Acha, E.M., Mianzan, H.W., Guerrero, R.A., Favero, M., Bava, J., 2004. Marine fronts at the continental shelves of austral South America: physical and ecological processes. *J. Mar. Syst.* 44, 83–105.
- Amante, C., Eakins, B.W., 2009. ETOPO1 1 Arc-minute Global Relief Model: Procedures, Data Sources and Analysis. NOAA Tech. Memor. NESDIS NGDC No. 24 (19 pp.).



- Bogazzi, E., Baldoni, A.N., Rivas, A., Martos, P., Reta, R.A., Orensanz, J.M., Lasta, M.L., Dell'Arciprete, P., Werner, F., 2005. Spatial correspondence between areas of concentration of Patagonian scallop (*Zygochlamys patagonica*) and frontal systems in the southwestern Atlantic. *Fish. Oceanogr.* 14, 359–376.
- Carreto, J.I., Lutz, V.A., Carignan, M.O., Colleoni, A.D.C., De Marco, S.G., 1995. Hydrography and chlorophyll-a in a transect from the coast to the shelf-break in the Argentinian Sea. *Cont. Shelf Res.* 15, 315–336.
- Carreto, J.I., Montoya, N.G., Carignan, M.O., Akselman, R., Acha, E.M., Derisio, C., 2016. Environmental and biological factors controlling the spring phytoplankton bloom at the Patagonian shelf-break front—degraded fucoxanthin pigments and the importance of microzooplankton grazing. *Prog. Oceanogr.* 146, 1–21.
- Carton, J.A., Giese, B.S., 2008. A reanalysis of ocean climate using Simple Ocean Data Assimilation (SODA). *Mon. Weather Rev.* 136, 2999–3017.
- Charo, M., Piola, A.R., 2014. Hydrographic data from the GEF Patagonia cruises. *Earth Syst. Sci. Data* 6, 265–271.
- Ciocco, N.F., Lasta, M.L., Narvarte, M., Bremec, C., Bogazzi, E., Valero, J., Orensanz, J.M., 2006. Fisheries and aquaculture: Argentina. In: Shumway, S.E., Parsons, G.J. (Eds.), *Scallops: Biology, Ecology and Aquaculture*. Elsevier, Amsterdam, pp. 1251–1283.
- Combes, V., Matano, R.P., 2014. A two-way nested simulation of the oceanic circulation in the southwestern Atlantic. *J. Geophys. Res.* 119, 731–756.
- Debreu, L., Marchesiello, P., Penven, P., Cambon, G., 2012. Two-way nesting in split-explicit ocean models: algorithms, implementation and validation. *Ocean Model* 49, 1–21.
- Dee, D.P., et al., 2011. The ERA-Interim reanalysis: configuration and performance of the data assimilation system. *Q. J. R. Meteorol. Soc.* 137, 553–597. <http://dx.doi.org/10.1002/qj.828>.
- Egbert, G.D., Erofeeva, S.Y., 2002. Efficient inverse modeling of barotropic ocean tides. *J. Atmos. Ocean. Technol.* 19, 183–204.
- Franco, B.C., 2013. Procesos acoplados bento-pelágicos relacionados con el establecimiento y deriva larval de la vieira patagónica (*Zygochlamys patagonica*) en el Océano Atlántico sudoeste. (Ph.D. Thesis) Universidad de Buenos Aires, Argentina (unpublished).
- Franco, B.C., Piola, A.R., Rivas, A.L., Baldoni, A., Pisoni, J.P., 2008. Multiple thermal fronts near the Patagonian shelf break. *Geophys. Res. Lett.* 35, L02607.
- Franco, B.C., Palma, E.D., Tonini, M.H., 2015. Benthic-pelagic uncoupling between the northern Patagonian frontal system and Patagonian scallop beds. *Estuar. Coast. Shelf Sci.* 153, 145–155.
- Franks, P.J.S., Chen, C., 1996. Plankton production in tidal fronts: a model of Georges Bank in summer. *J. Mar. Res.* 54, 631–651.
- Gaston, G.R., 1987. Benthic Polychaeta of the Middle Atlantic Bight: feeding and distribution. *Mar. Ecol. Prog. Ser.* 36, 251–262.
- Gawarkiewicz, G., Chapman, D.C., 1992. The role of stratification in the formation and maintenance of shelf break fronts. *J. Phys. Oceanogr.* 22, 753–772.
- Graf, G., 1992. Benthic–pelagic coupling: a benthic view. *Oceanogr. Mar. Biol.* 30, 149–190.
- Grebmeier, J.M., Barry, J.P., 1991. The influence of oceanographic processes on pelagic-benthic coupling in polar regions: a benthic perspective. *J. Mar. Syst.* 2, 495–518.
- Heip, C.H.R., et al., 2001. The role of the benthic biota in sedimentary metabolism and sediment-water exchange processes in the Goban Spur area (NE Atlantic). *Deep-Sea Res. II* 48, 3223–3243.
- Hily, C., 1991. Is the activity of benthic suspension feeders a factor controlling water quality in the Bay of Brest? *Mar. Ecol. Prog. Ser.* 69, 179–188.
- Josefson, A.B., Conley, D.J., 1997. Benthic response to a pelagic front. *Mar. Ecol. Prog. Ser.* 147, 49–62.
- Ledwell, J.R., Watson, A.J., Law, C.S., 1998. Mixing of a tracer in the pycnocline. *J. Geophys. Res.* 103, 21499–21529.
- Loder, J.W., Perry, R.I., Drinkwater, K.F., Grant, J., Harding, G.C., Harrison, W.G., Horne, E.P.W., Oakey, N.S., Taggart, C.T., Tremblay, M.J., Brickman, D., Sinclair, M.M., 1992. Physics and biology of the Georges Bank frontal system. In: *Science Review of the Bedford Institute of Oceanography, Halifax Fisheries Research Laboratory, and St. Andrews Biological Station*. Department of Fisheries and Oceans, Canada, pp. 57–61.
- Lutz, V.A., Segura, V., Dogliotti, A.I., Gagliardini, D.A., Bianchi, A.A., Balestrini, C.F., 2010. Primary production in the Argentine Sea during spring estimated by field and satellite models. *J. Plankton Res.* 32, 181–195.
- Marra, J., Houghton, R.W., Garside, C., 1990. Phytoplankton growth at the shelf-break front in the Middle Atlantic Bight. *J. Mar. Res.* 48, 851–868.
- Matano, R.P., Palma, E.D., 2008. On the upwelling of downwelling currents. *J. Phys. Oceanogr.* 38, 2482–2500.
- Mauna, A.C., Botto, F., Franco, B.C., Schwartz, J.M., Acha, E.M., Lasta, M.L., Iribarne, O.O., 2011. Shifts in an epibenthic trophic web across a marine frontal area in the southwestern Atlantic (Argentina). *J. Sea Res.* 66, 248–255.
- Menge, B.A., Daley, B.A., Wheeler, P.A., Dahloff, E., Sanford, E., Strub, P.T., 1997. Benthic–pelagic links and rocky intertidal communities: bottom-up effects on top-down control? *Proc. Natl. Acad. Sci.* 94, 14530–14535.
- Piola, A.R., Avellaneda, N.M., Guerrero, R.A., Jardón, F.P., Palma, E.D., Romero, S.I., 2010. Malvinas-slope water intrusions on the northern Patagonia continental shelf. *Ocean Sci.* 6, 345–359.
- Piola, A.R., Franco, B.C., Palma, E.D., Saraceno, M., 2013. Multiple jets in the Malvinas Current. *J. Geophys. Res. Oceans* 118, 2107–2117.
- Pringle, J.M., Franks, P.J.S., 2001. Asymmetric mixing transport: a horizontal transport mechanism for sinking plankton and sediment in tidal flows. *Limnol. Oceanogr.* 46, 381–391.
- Romero, S.I., Piola, A.R., Charo, M., Garcia, C.A.E., 2006. Chlorophyll-a variability off Patagonia based on SeaWiFS data. *J. Geophys. Res.* 111, C05021.
- Ross, O.N., Sharples, J., 2004. Recipe for 1-d Lagrangian particle tracking models in space-varying diffusivity. *Limnol. Oceanogr. Methods* 2, 289–302.
- Ross, O.N., Sharples, J., 2008. Swimming for survival: a role of phytoplankton motility in a stratified turbulent environment. *J. Mar. Syst.* 70, 248–262.
- Saraceno, M., Provost, C., Piola, A.R., 2005. On the relationship between satellite retrieved surface temperature fronts and chlorophyll-a in the western South Atlantic. *J. Geophys. Res.* 110, C11016.
- Schejter, L., Bremec, C., Akselman, R., Hernández, D., Spivak, E.D., 2002. Annual feeding of the Patagonian scallop *Zygochlamys patagonica* (King and Broderip, 1832) in Reclutas bed (39°S–55°W), Argentine Sea. *J. Shellfish Res.* 21, 549–555.
- Schlag, Z.R., North, E.W., Smith, K.A., 2008. Larval TRANSPORT Lagrangian Model (LTRANS) User's Guide. University of Maryland Center for Environmental Science Horn Point Laboratory Technical Rep (146 pp.).
- Sharples, J., Moore, C.M., Hickman, A.E., Holligan, P.M., Tweddle, J.F., Palmer, M.R., Simpson, J.H., 2009. Internal tidal mixing as a control on continental margin ecosystems. *Geophys. Res. Lett.* 36, L23603. <http://dx.doi.org/10.1029/2009GL040683>.
- da Silva, A.M., Young, C.C., Levitus, S., 1994. Atlas of surface marine data 1994. In: *Vol. 1: Algorithms and Procedures NOAA Atlas NESDIS No 8* (83 pp.).
- Simpson, J.H., Souza, A.J., 1995. Semidiurnal switching of stratification in the region of freshwater influence of the Rhine. *J. Geophys. Res.* 100, 7037–7044.
- Soria, G., Orensanz, J.M., Morsán, E.M., Parma, A.M., Amoroso, R.O., 2016. Scallops biology, fisheries, and management in Argentina. In: Shumway, S.E., Parsons, G.J. (Eds.), *Scallops: Biology, Ecology, Aquaculture, and Fisheries*. Elsevier, Amsterdam, pp. 1019–1046.
- Thorpe, S.A., 2005. *The Turbulent Ocean*. Cambridge University Press, New York (484 pp.).
- Tian, R., Chen, C., Qi, J., Ji, R., Beardsley, R.C., Davis, C., 2015. Model study of nutrient and phytoplankton dynamics in the Gulf of Maine: patterns and drivers for seasonal and interannual variability. *ICES J. Mar. Sci.* 72, 388–402.
- Valla, D., Piola, A.R., 2015. Evidence of upwelling events at the northern Patagonian shelf break. *J. Geophys. Res.* 120, 7635–7656.
- Visser, A.W., 1997. Using random walk models to simulate the vertical distribution of particles in a turbulent water column. *Mar. Ecol. Prog. Ser.* 158, 275–281.
- Wing, S.R., Botsford, L.W., Largier, J.L., Morgan, L.E., 1995. Spatial structure of relaxation events and crab settlement in the northern California upwelling system. *Mar. Ecol. Prog. Ser.* 128, 199–211.